J MATER SCI **41** (2006) 1523–1527

Iron at earth-core conditions

P. MODAK, A. K. VERMA, R. S. RAO, B. K. GODWAL
High Pressure Physics Division, Bhabha Atomic Research Centre, Trombay, Mumbai 400 085, India
E-mail: pmodak@magnum.barc.ernet.in

R. JEANLOZ*
Department of Earth and Planetary Science, University of California, Berkeley, USA

We have carried out electronic structure calculations for iron under high pressure using pseudopotential plane wave methods. There is a controversy regarding the structure of iron at moderate pressures (30–100 GPa) and temperatures (1000–2400 K), with different experiments suggesting different structures, such as orthorhombic, double hexagonal close packed (dhcp), etc. Our earlier calculations using the linear muffin-tin orbital method within atomic-sphere-approximation had argued against the stability of the orthorhombic phase. The more accurate calculations presented here predict qualitatively the same results. We have additionally studied the stability of various phases of Fe at different compressions by calculating phonon frequencies. These rule out the stability of the orthorhombic phase. To validate our zero-temperature electronic-structure results at finite temperature, we have compared the shock Hugoniot and melting properties of iron with the results of our electronic structure calculations. Though we have used simplified models for these estimates, our predictions compare well with the experimental data. We thus propose that these models can be used to obtain the information about the high-pressure melting curves of planetary materials.

1. Introduction

High-pressure and high-temperature physical properties of solid are of great importance in many fields in science, and in particular solid and molten iron play a central role in geophysics as iron forms a major part of the Earth's core. Note that the seismological measurements of elastic wave velocities show that Earth's core has an average atomic number of about 25, close to that of iron. The Earth's core extends to about 2900 km from the surface and stores a substantial part of the planet's energy, thus significantly influencing internal dynamic processes. Seismic data reveal that the core contains a solid inner core and a liquid outer core. There are seismological observations that compressional waves that traverse the inner core travel 3 to 4% faster along Earth's spin axis than in the equatorial plane, thus indicating an elastically anisotropic inner core. The conventional interpretation of this anomaly is based on the idea of a partial alignment of crystals of hexagonal close packed (hcp) Fe [1].

The phase diagram of Fe has been studied extensively [2] because of its geophysical importance. In general, there is consensus regarding the moderate pressure and temperature phase diagram of Fe, with body centered cubic (bcc)-Fe stable at ambient conditions, hcp-Fe stable above about 15 GPa at low temperatures, and the face centered cubic (fcc) structure being stable above about 1300 K at low pressures. Some high-pressure, high-temperature diamond anvil cell experiments [3, 4] suggest the occurrence of a new phase (β) above ~40 GPa and ~1,000 K; but the structure of this new phase is still unresolved as different sets of experimental data suggest different structures [3, 4]. Saxena and co-workers indexed the diffraction pattern on a double hexagonal close packed (dhcp) structure for samples quenched from the temperature range 1,500–2,200 K at 30–60 GPa [3]. However, Andrault *et al* concluded that iron goes to an orthorhombic structure in the pressure range 30–100 GPa and at high temperature (2375) K [4].

*Author to whom all correspondence should be addressed.
0022-2461
DOI: 10.1007/s10853-006-4620-5

We had earlier studied the relative phase stability of iron [5] by the linear muffin-tin orbital (LMTO) method with atomic sphere approximation (ASA) [6, 7]. Our detailed comparison of the calculated total energies of fcc, hcp, dhcp, orthorhombic, and monoclinic (with two atoms/cell, which could be in the transit path of hcp- fcc) structures, along with considerations of the entropy contributions to free energy had indicated that the phase observed by Andrault *et al* was not likely to have been the orthorhombic structure that we examined.

With the controversy of this high-pressure, high-temperature phase of iron still persisting, and in view of the accuracy limitations involved in the LMTO-ASA method, we have recently re-investigated the relative phase stabilities of bcc, hcp, and orthorhombic (Pbcm) phases by calculations using an accurate ultrasoft pseudopotential. As we show below, these more accurate calculations lead qualitatively to the same results, though differ somewhat in quantitative details. We have also studied the lattice dynamical properties of bcc, hcp and orthorhombic phases within the density functional perturbation theory as implemented in the PWSCF code [8], and find that at high pressure both bcc and orthorhombic phases are elastically unstable (i. e., some of the mode frequencies become negative). If thermal effects are neglected at ambient pressure, the calculated phonon dispersions for bcc phase agree well with available experimental data [9]. The phonon dispersions for the hcp phase remain unaltered under pressure, except for a small change along the K-M direction and the known hardening of the modes. To validate our 0 K results at finite temperature, we calculated the shock Hugoniot and melting curve using 0 K total energies, and find that our theoretical results match very well with existing experimental shock data. The melting curve as a function of pressure is obtained according to a recently published model based on dislocation mediated melting [10], and also compared with results based on the Lindemann criterion [11]. The shock melting point which is taken as the intersection of these curves with the Hugoniot matches well with that previously estimated from the shock measurements [12].

2. Details of calculations

The details of the methods used to estimate the thermal contributions to the isotherm and Hugoniot for solids are well documented in the literature [13, 14], and we summarize here only the key aspects of the formulation. Briefly, we have evaluated the internal energy at various volumes as a sum of three terms,

$$E = E_c + E_{lat} + E_{ele}.$$

where E_c represents the 0 K (cold) total energy, E_{lat} the vibrational energy of the ions, and E_{ele} the energy due to thermal excitation of electrons. We have used the plane wave self-consistent field (PWSCF) method with generalized gradient approximation (GGA) [15] for exchange-correlation energy to calculate E_c. The plane-wave calculations were carried out with an ultrasoft pseudopotential with $3d^7 4s^1$ as valence configuration. For the plane-wave expansion we take 25 Ry as the energy cutoff. We use 290 **k**-points for the bcc, and 146 **k**-points for orthorhombic, hcp and dhcp structures for sampling the irreducible wedge of the Brillouin zone (BZ). E_{lat} and E_{ele} are evaluated by using the relations shown below [13, 14]:

$$E_{lat} = 3k_B T\, \mathcal{D}(\theta_D/T),$$
$$E_{ele} = 0.5\beta\, T^2,$$

where β represents the electronic specific heat, $\mathcal{D}$ (θ_D/T) is the Debye function, and θ_D is the Debye temperature; T and k_B are temperature and Boltzmann's constant, respectively. The lattice vibrational energy is estimated using the Debye-Mie Grüneisen model, which is based on the assumption that the vibrational energy levels of ions are the same as those of harmonic oscillators [16]. The electronic thermal excitation energy is estimated by the free-electron formula using density of states at the Fermi level obtained by our PWSCF calculations. The corresponding equation for pressure is given by [17, 13]

$$P = -\triangle E_c/\triangle V + \gamma_{lat} E_{lat}/V + \gamma_{ele} E_{ele}/V,$$

where,

$$P_{ele} = \gamma_{ele} E_{ele}/V,$$
$$P_{lat} = \gamma_{lat} E_{lat}/V,$$

γ_{ele} and γ_{lat} being the electronic and lattice Grüneisen parameters. In addition, γ_{lat} (P) under pressure (P) at density (ρ) was obtained by

$$\gamma_{lat}(P) = \gamma_{lat}(0)\rho_0/\rho + 2/3(1 - \rho_0/\rho)$$

The solid Hugoniot (locus of all states that reached by a single shock from a given initial state) is obtained by solving self-consistently the following conservation equation for the internal energy:

$$E - E_0 = (P + P_0)(V_0 - V)/2,$$

where E, P, V refer to the shocked material, and E_0, P_0, V_0 refer to the unshocked material.

The melting curves under pressure are obtained by two methods, i.e.,

(i) Lindemann Law

This is based on the hypothesis that elements melt when the amplitude of atomic vibration is a fixed fraction, $\cong$1/8,

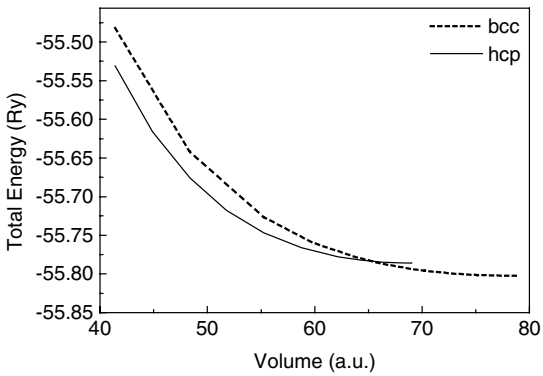

Figure 1 Calculated cold energy-volume relations for bcc and hcp Fe.

TABLE I Comparison of the calculated physical quantities of iron and experimental data

Properties	Our calculations	Experimental [21]
Bcc Fe		
Equlibrium volume	78.732 (a.u.)	79.170 (a.u.)
Bulk modulus (B)	179.6 (GPa)	173 (GPa)
Pressure derivative of B	3.66	5.0
Magnetic moment	2.38 μ_B/cell	2.12 μ_B/cell
Hcp Fe		Other calculations [7]
Equlibrium volume	68.96 (a.u.)	68.86 (a.u.)
Bulk modulus (B)	298.7 (GPa)	291 (GPa)
Pressure derivative of B	3.55	4.4
Magnetic moment	0.0	0.0

of the interatomic distance [11]. The melting temperature $T_m(P)$ at pressure P is then given by

$$T_m(P) = T_m(0) \quad (V/V_0)^{2/3} \quad \exp[2\gamma_{lat}(1 - V/V_0)],$$

where $T_m(0)$ is the ambient pressure melting temperature.

(ii) Dislocation -mediated melting

In this case, the solid to liquid transition is modeled as a transition from a translationally symmetric (ordered) to a translationally disordered system, and the order-disorder transition temperature is taken as the melting temperature [10]. The melting temperature at pressure P is then determined by,

$$G[P, T_m(P)] \quad \nu_{WS}[P, T_m(P)]/T_m(P) = \text{const.}$$

Under the assumptions that the shear modulas (G) and Wigner-Seitz volume (ν_{WS}) are weakly dependent on temperature (i.e., respective higher temperature values are taken equal to the values at room temperature) the following relation can be derived,

$$T_m(P) = T_m(0)(1 + PB'/B)^{-(1/B')} [1 + PG'/G(1 + PB'/B)^{-(1/3B')}], \quad \text{with} \quad P \leq 2B$$

where B, G are ambient-condition bulk and shear modulii, respectively, and B′, G′ are the first pressure derivatives of the respective quantities at ambient pressure [18].

3. Results and discussion

In Table I, we give calculated equilibrium volume, bulk modulus, and its pressure derivative both for bcc and hcp phases of iron, which we obtained by fitting our calculated total energies to the Birch-Murnaghan equation of state. These results are in good agreement with experiments [19, 20] and earlier calculations [21–23].

Fig. 1 depicts the comparison of first-principles calculated 0-K total energies between hcp and bcc phases of iron as a function of volume per atom, and thus shows the stability region of these two phases which is consistent with the existing literature [22]. We have also calculated total energies for fcc, dhcp and orthorhombic phases, and found that for dhcp and fcc phases they are very close to that of the hcp phase (∼3–4 mRy), and that of orthorhombic phase is about 5 mRy higher than the hcp energy. Also our 0-K geometry optimization for the orthorhombic structure shows that it is not elastically stable; in fact it transforms to the hcp structure. These results are consistent with the high pressure phonon frequency calculations which show that some modes give negative frequencies in the bcc and orthorhombic structures, thus confirming their elastic instability. Note that at ambient pressure the phonon frequencies as shown in Table II match well with the experimental data of Brockhouse *et al.* obtained from inelastic neutron scattering measurements [9]. Moreover the reliability of our calculations have been confirmed by comparing the phonon frequencies (Fig. 2) in the hcp structure with those of Söderlind *et al.* obtained by FP-LMTO based calculations [23]. Hence our calculations argue against the stability of the orthorhombic phase at 0-K, and also at high temperature because it is unlikely that the thermal contributions will compensate the energy differences of 10 mRy [5].

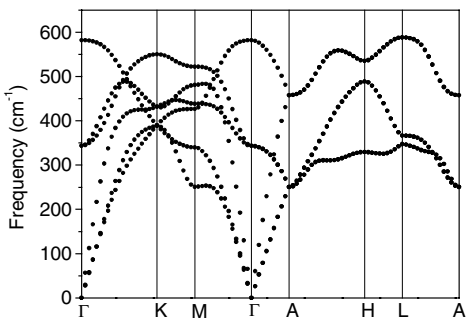

Figure 2 Calculated phonon dispersion of non-magnetic hcp Fe at 212 GPa pressure along the different high symmetry directions of BZ.

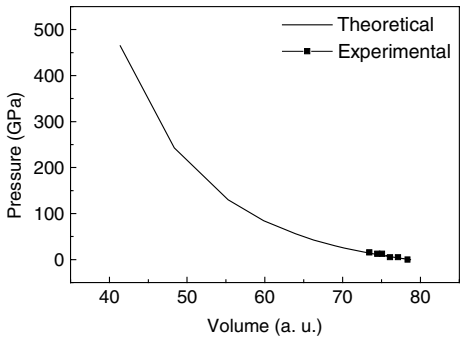

(a)

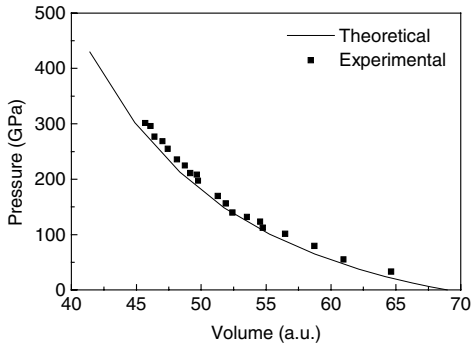

(b)

Figure 3 Calculated Equation of states for (a) bcc Fe (b) hcp Fe. Experimental data are from Jephcoat *et al*. [19] and Mao *et al*. [20].

In Figs 3a and b we compare our P-V isotherm (including room temperature effects) calculated in magnetic bcc and non-magnetic hcp phases respectively along with the available experimental (DAC) data. It is clearly seen that at low pressures our P-V curve is in agreement with the data of Jephcoat *et al*. [19] while at higher compressions it agrees with those of Mao *et al*. [20].

We have also studied the magnetic moment of the bcc phase as a function of compression. We observe that the magnetic moment of the bcc structure decreases with compression (Fig. 4), and at around a volume compression of 0.51 the magnetic moment becomes 0.60 μ_B, in good agreement with the earlier full-potential LMTO calculations [23]. The collapse of magnetic moment can be understood in terms of the decrease of density of states at the Fermi level under pressure. Therefore, the bcc phase

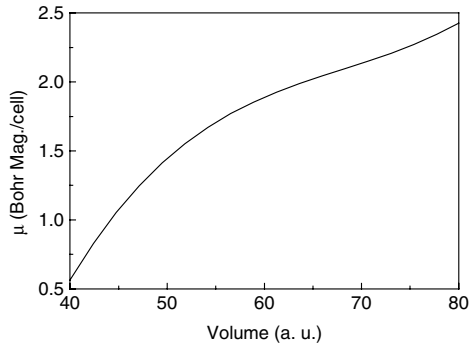

Figure 4 Calculated variation of Magnetic moment of bcc Fe with compression. Calculated equilibrium volume is 78.73 a. u.

could have an appreciable magnetic moment in the Earth's core, and hence it has been argued that because of magnetic entropy the bcc phase may be more stable than the non-magnetic hcp phase [21].

However our EOS results and their comparison with the experimental data (see Fig. 3) do not support this view.

Fig. 5 shows the comparison of calculated solid Hugoniot with the experimental data obtained by Brown *et al*. [12]. For shock Hugoniot calculations we have used 0-K isotherm, lattice and electronic Grüneisen parameters along with thermal contributions of bcc phase up to $V/V_0 = 0.8$ and of hcp phase for higher compressions, in accordance with the stability of these phases discussed earlier. It is seen from Fig. 5 that our calculated solid Hugoniots are in excellent agreement with experimental data [12].

Fig. 6 shows our calculated Hugoniot curve in the P-T plane along with the melting curves calculated from the Lindemann law and dislocation-mediated melting model.

Our calculated melting temperatures (T_m) are 4803 K at P = 229 GPa (Lindemann Law) and 9251 K at P = 388 GPa (dislocation mediated melting for bcc-Fe). Dislocation mediated melting curve in the bcc phase is in better agreement with laser heated Diamond-anvil cell (DAC) data of Williams *et al*. [24]. However both these melting curves differ with the melting data of Boehler *et al*. [25]. It may be noted that the shock melting is underestimated by the Lindemann law. However our calculated solid Hugoniot compare well with the Brown *et al*'s experimentally-based estimate of Hugoniot P-T data even

TABLE II Comparison of phonon frequencies for magnetic bcc phase along [111] symmetry direction of BZ with that of neutron inelastic measurements of Brokhouse *et al*. [9]

ξ		0.125	0.250	0.375	0.500	0.625	0.750	0.875
Theoretical [$\xi\xi\xi$]	ν(T) (THz)	2.13	4.25	5.91	6.90	7.50	7.93	8.20
	ν(L) (THz)	4.18	7.25	8.03	6.90	5.69	5.65	7.22
Experimental [$\xi\xi\xi$]	ν(T) (THz)	2.22 ±0.06	4.56 ±0.06	6.26 ±0.06	7.15 ±0.08	7.90 ±0.10	8.24 ±0.10	8.40 ±0.25
	ν(L) (THz)	4.52 ±0.08	7.72 ±0.08	8.38 ±0.11	7.15 ±0.08	5.78 ±0.08	6.22 ±0.08	7.72 ±0.10

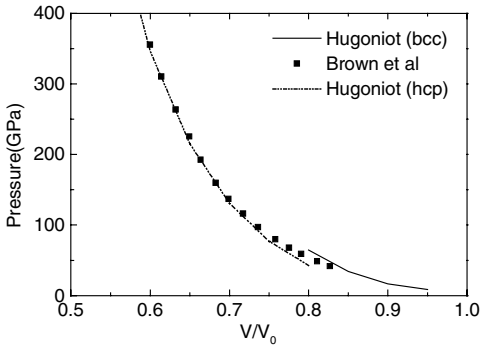

Figure 5 Calculated solid Hugoniot of iron for bcc and hcp phases. Experimental data are from Brown *et al*. [12]. V_0 is the volume under ambient condition.

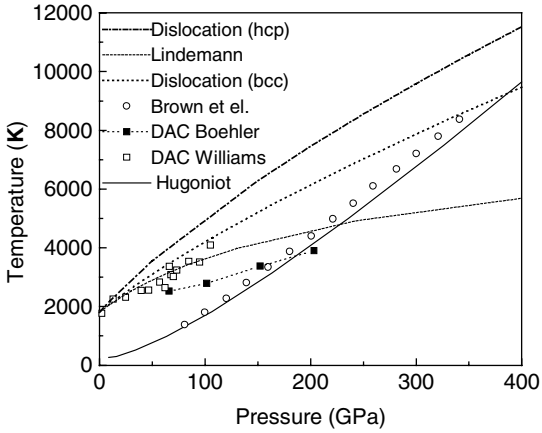

Figure 6 Calculated P-T Hugoniot, and melting curves based on Lindmann law, and dislocation mediated melting for bcc and hcp phases. Experimental results are from Brown *et al*. [12] , Williams et al. [24] and Boehler [25].

above 229 GPa pressure. For comparison we have also shown in Fig. 6 the melting curve for the hcp-Fe based on dislocation mediated model, which gives much higher melting temperature.

4. Conclusions

We can conclude based on our first-principles electronic-structure and phonon calculations that the orthorhombic phase of iron is not stable at any pressure, over the range examined, at zero temperature. It is also unlikely that the thermal contributions will be able to compensate for the energy difference of about 5 mRy, relative to other structures, at high temperature. This is consistent with the findings from energy-dispersive experiments [26] with double-sided laser heating in the diamond-anvil cell (for reducing thermal gradients) which do not support the presence of an orthorhombic phase. For Hugoniot and melting calculations we have used simple models, but their estimates are close to the experimental data. Hence these models can be used to predict melting at high-pressures conditions, for which experimental measurements and *ab initio* calculated results may otherwise be difficult to obtain.

References

1. L. STIXRUDE and R. E. COHEN, *Nature* **267** (1995) 1972.
2. See, for example, In High-Pressure Science and Technology-1993, edited by S. C. Schmidt, J. W. Shaner, G. A. Samara and M. Ross (American Institute of Physics, New York, 1994) p. 887.
3. S. K. SAXENA, L.S. DURBOVINSKY, P. HAGGKVIST, Y. CERENIUS, G. SHEN and H. K. MAO, *Science* **269** (1995) 1703.
4. D. ANDRAULT, G. FIQUET, M. KUNZ, F. VISOCEKAS and D. HAUSERMANN, *Science* **278** (1997) 831.
5. R. S. RAO, P. MODAK, B. K. GODWAL and S. K. SIKKA, *Phys. Rev.* B **59** (1998) 13498.
6. O. K. ANDERSEN, *ibid.* B **12** (1973) 3060.
7. H. L. SKRIVER, "The LMTO Method" (Springer, Berlin 1984).
8. S. BARONI, S. DE GIRONCOLI, A. D. CORSO and P. GIANNOZZI, *Rev. Mod. Phys.* **73** (2001) 515.
9. B. N. BROCKHOUSE, H. E. ABOU-HELAL and E. D. HALLMAN, *Solid State Commun.* **5** (1967) 211.
10. L. BURAKOVSKY, D. L. PRESTON and R. R. SILBAR, *Phys. Rev.* B **41** (1990) 7440.
11. F. A. LINDEMANN, *Z. Phys.* **11** (1910) 609.
12. J. M. BROWN and R. MCQUEEN, *J. Geophys. Res* **91** (1986) 7485.
13. B. K. GODWAL, S. K. SIKKA and R. CHIDAMBARAM, *Phys. Rep* **102** (1983) 121.
14. B. K. GODWAL and R. JEANLOZ, *Phys. Rev.* B **41** (1990) 7440.
15. J. P. PERDEW, K. BURKE and M. ERNZERHOF, *Phys. Rev. Lett.* **77** (1996) 3865.
16. YA. B. ZEL'DOVICH and YU. P. RAIZER, "Physics of shock waves and High Temprature Hydrodynamics Phenomena", (Academic Press, NY 1976).
17. R. S. HIXSON and J. N. FRITZ, *J. Appl. Phys.* **71** (1992) 1721.
18. For a more accurate formulations of melting curve based on the dislocation mediated melting, see A. B. BELONOSHKO, S. I. SINAK, A. E. KOCHETOV, B. JOHANSSON, L. BURAKOVSKY and D. L. PRESTON, *Phys. Rev. Lett.* **92** (2004) 195701.
19. A. P. JEPHCOAT, H. K. MAO and P. M. BELL, *J. Geophys. Res.* **91** (1986) 4677.
20. H. K. MAO, Y. WU, L.C. CHEN, J.F. SHU and A. P. JEPHCOAT, *J. Geophys. Res* **95** (1990) 21737.
21. L. VOCADLO, J. BRODHOLT, D. ALFE', M. J. GILLAN and G. D. PRICE, *Phys. Earth Planet. Inter.* **117** (2000) 123.
22. L. STIXRUDE, R. E. COHEN and D. J. SINGH, *Phys. Rev.* B **50** (1994) 6442.
23. P. SÖDERLIND, J. A. MORIARTY and J. M. WILLIS, *ibid.* B **53** (1996) 14063.
24. Q. R. WILLIAMS, R. JEANLOZ, J. BASS, B. SVENDSEN and T. J.AHRENS, *Science* **236** (1987) 181.
25. R. BOEHLER, *Nature* (London) **363** (1993) 534 .
26. G SHEN, H. K. MAO, R. J. HEMLAY, T. S. DUFFY and M. L. RIVERS, *J. Geophys. Res. Lett* **25** (1998) 373.

Received 14 May 2004
and accepted 22 April 2005